Journal of Sound and Vibration (1997) **208**(5), 841–859

ENERGY FLOW ANALYSIS OF VIBRATING BEAMS AND PLATES FOR DISCRETE RANDOM EXCITATIONS

F. Han, R. J. Bernhard and L. G. Mongeau

Ray W. Herrick Laboratories, School of Mechanical Engineering, Purdue University, West Lafayette, Indiana 47907-1077, *U.S.A.*

(*Received* 10 *March* 1997, *and in final form* 15 *July* 1997)

Two methods for calculating the power input to vibrating beams and plates excited by multiple discrete random forces are developed. The power input is expressed in terms of the cross-power spectral density between the exciting forces. An approximate energy density solution is obtained using energy flow analysis. The power input calculations and the energy density response predictions are verified using modal analysis for different coherence conditions between the random excitation forces.

1. INTRODUCTION

The energy flow analysis method (EFA), and its finite element approximation, the energy finite element method (EFEM), allow computationally efficient predictions of the spatially and frequency averaged response of structural acoustic systems. Previous investigations of the application of EFA to the vibration of rods and beams were reported by Wohlever and Bernhard [1]. The approach was also applied to membranes and plates by Bouthier and Bernhard [2, 3], and to acoustic enclosures by Bouthier [4]. These derivations assume diffuse wave fields based on the superposition of lossy plane waves. The resulting equations of motion, cast in terms of energy variables, are similar to those derived by Rybak and his colleagues [5–8] using the assumption of incoherent scattered waves. They are also similar to those obtained from the so-called Simple Energy Formulation, derived by LeBot [9], which can itself be derived by spatially averaging exact expressions for the energetics of the structure (the General Energy Formulation).

These methods have been verified both analytically and experimentally for simple harmonic excitations, and for local random forces. For many applications, however, the structure may be excited simultaneously by many local random forces, which may be incoherent or partially coherent. In this study, two methods for calculating the input power required for the estimation of the energy response of the structure for partially coherent forces are derived and compared: a transfer function method and an impedance method. Energy flow predictions are obtained for beams and plates using EFA and both power input calculation methods. The results are compared with classical displacement solutions obtained using modal analysis for the case of two random forces.

2. POWER INPUT TO BEAMS AND PLATES

The equations governing the energy distribution associated with the progagation of flexural waves in a transversely vibrating beam were derived by Wohlever and Bernhard

0022–460X/97/500841 + 19 $25.00/0/sv971205

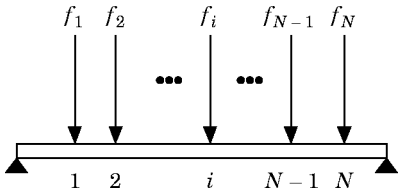

Figure 1. A beam excited by N discrete random forces.

[1] for free vibrations. As shown by Bouthier and Bernhard [2], the inhomogeneous form of the energy flow analysis equation for the case in which there is a power input to the beam is

$$-\frac{c_g^2}{\eta\omega}\frac{\mathrm{d}^2 e}{\mathrm{d}x^2} + \eta\omega e = \pi_{in}(x), \tag{1}$$

where e is the far field, time-averaged, "smoothed" energy density, c_g is the group velocity of flexural waves, η is the loss factor, and $\pi_{in}(x)$ is the power input per unit length. For thin, transversely vibrating plates, where the wave field can be assumed to be a superposition of plane waves, the governing equation is similar, but two-dimensional [2],

$$-\frac{c_g^2}{\eta\omega}\nabla^2 e + \eta\omega e = \pi_{in}(x, y), \tag{2}$$

where $\nabla^2 = \partial^2/\partial x^2 + \partial^2/\partial y^2$, and $\pi_{in}(x,y)$ is the power input per unit area.

Previous work on EFA [1–4] has shown that the high frequency energy density response of a vibrating system obtained from EFA is in good agreement with the response predicted by exact methods, such as modal analysis, for one single local exciting force. The case of multiple, local random exciting forces is treated in the following. A simply supported beam and a simply supported plate will be considered, as illustrated in Figures 1 and 2, respectively. An arbitrary number, N, of discrete random forces, which may be coherent, incoherent or partially coherent with each other, are exerted on the structure. Two methods to evaluate the power input were developed: a transfer function method and an impedance method.

2.1. THE TRANSFER FUNCTION METHOD

The input forces and the velocity response of the structure are assumed to be stationary random processes. For a finite time interval $0 \leqslant t \leqslant T$, the cross-spectrum between the

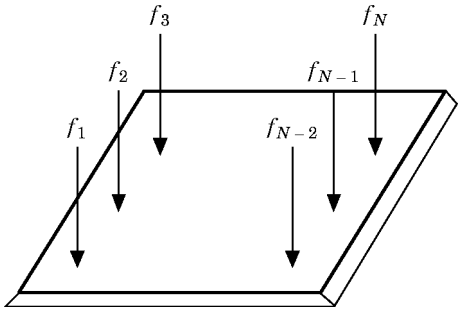

Figure 2. A plate excited by N discrete random forces.

input force and the velocity at point i is [11]

$$S_{fv,i}(\omega, T, n) = \frac{1}{T} F_i(\omega, T, n) V_i^*(\omega, T, n), \tag{3}$$

where

$$F_i(\omega, T, n) = \int_0^T f_i(t, n)\, \mathrm{e}^{-\mathrm{j}\omega t}\, \mathrm{d}t \tag{4}$$

and

$$V_i(\omega, T, n) = \int_0^T v_i(t, n)\, \mathrm{e}^{-\mathrm{j}\omega t}\, \mathrm{d}t. \tag{5}$$

In equations (4) and (5), f_i and v_i are the force and the velocity at point i, respectively, the asterisk represents the complex conjugate operator, the quantities F_i and V_i represent finite Fourier transforms, and n is the ensemble index. The power input spectral density to point i can be obtained from the cross-spectral density function between force and velocity, given by

$$\pi_{in,i} = \mathrm{Re}\,[S_{fv,i}(\omega)] = \mathrm{Re}\left[\lim_{T\to\infty} \mathrm{E}\{S_{fv,i}(\omega, T, n)\}\right], \tag{6}$$

where $\mathrm{E}\{\ \}$ denotes the expectation over the ensemble index n. The velocity at point i has contributions from all N forces. Therefore, V_i can be written as

$$V_i(\omega, T, n) = \sum_{j=1}^{N} H_{ij}(\omega) F_j(\omega, T, n), \tag{7}$$

where H_{ij} is the transfer function between the excitation f_j at point j and the velocity response at point i. Substituting equation (7) into equation (3) and then equation (6) yields the power input spectral density at point i:

$$\pi_{in,i} = \sum_{j=1}^{N} \mathrm{Re}\,[S_{ij}(\omega) H_{ij}^*(\omega)], \tag{8}$$

where S_{ij} is the cross-spectral density between forces at points i and j.

This power input calculation method is exact. From a modal description of the structural response, the transfer function can be expressed as a summation of modes as

$$H_{ij}(\omega) = \frac{\mathrm{j}\omega}{m} \sum_{r=1}^{\infty} \frac{\phi_r(x_i)\phi_r(x_j)}{\omega_r^2 - \omega^2(1 - \mathrm{j}\eta)}, \tag{9}$$

where ϕ_r is the eigenfunction for the rth mode, ω_r is the natural frequency, and m is the mass per unit length for the case of the beam, or the mass of unit area for the case of the plate. The transfer function, a truncated infinite series, requires significant computational effort, since many modes must be included for high frequency predictions.

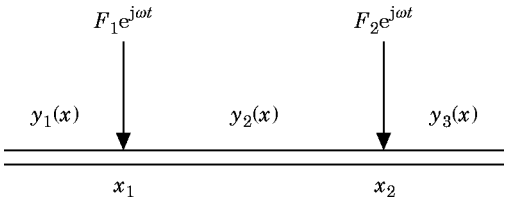

Figure 3. An infinite beam excited by two simple harmonic forces.

2.2. THE IMPEDANCE METHOD

As an alternative approach, the input impedance of the actual structure may be approximated by that of a comparable structure of infinite extent. This method will be referred to as the impedance method. For one single mechanical source, the power input at one point is [10]

$$\pi_{in} = \frac{|f|^2}{2} \operatorname{Re}\left(\frac{1}{Z_m}\right), \tag{10}$$

where Z_m is the impedance at the driving point. If the impedance of an infinite system is used to approximate the exact impedance,

$$\pi_{in} \approx \tfrac{1}{2}|f|^2 \operatorname{Re}\left(\frac{1}{Z_\infty}\right). \tag{11}$$

The impedance of an infinitely long beam excited by a local force is [10]

$$Z_\infty = 2(1+\mathrm{j})(EI)^{1/4}\omega^{1/2}(\rho A)^{3/4} = 2(1+\mathrm{j})EI\omega^{-1}k^3, \tag{12}$$

where EI is the flexural rigidity, k is the wavenumber, ρ is the beam density, and A is the cross-sectional area. The impedance of an infinite plate is [10]

$$Z_\infty = 8(D\rho h)^{1/2}, \tag{13}$$

where D is the bending stiffness, and ρh is the mass of the plate per unit area. The impedance of a finite beam or plate varies significantly from the impedance of an infinite beam or plate at low frequencies, and thus the use of equation (11) in place of equation (10) may cause significant errors. However whenever high frequencies and the spatially averaged response are considered, the impedance of an finite system is known to approach that of an infinite system. In this situation, the approximation is reasonable.

For multi-point excitation the calculation of power input is not as straightforward as equation (11) because of the interaction between the excitation forces. The simple case of an infinitely long beam excited by two simple harmonic forces will be used to illustrate the behavior of multiple force systems. The beam is shown in Figure 3. Assuming one-dimensional flexural wave propagation in the beam and incorporating the energy dissipation by using a complex wavenumber, the displacement of the beam can be expressed analytically from a travelling wave solution. The displacement in each region is given by [10]

$$\begin{cases} y_1(x) = B_1\, \mathrm{e}^{\mathrm{j}\mathbf{k}x} + D_i\, \mathrm{e}^{\mathbf{k}x}, & x \leqslant x_1, \\ y_2(x) = A_2\, \mathrm{e}^{-\mathrm{j}\mathbf{k}x} + B_2\, \mathrm{e}^{\mathrm{j}\mathbf{k}x} + C_2\, \mathrm{e}^{-\mathbf{k}x} + D_2\, e^{\mathbf{k}x}, & x_1 \leqslant x \leqslant x_2, \\ y_3(x) = A_3\, \mathrm{e}^{-\mathrm{j}\mathbf{k}x} + C_3\, \mathrm{e}^{-\mathbf{k}x}, & x \geqslant x_2, \end{cases} \tag{14}$$

where $\mathbf{k}$ is the complex wavenumber, and x_1 and x_2 are the locations of the two forces. Using the joint conditions at x_1 and x_2 with equation (14) yields

$$\begin{aligned} y_1(x) &= \frac{1}{4\mathbf{E}I\mathbf{k}^3}(-\mathrm{j}F_1\,\mathrm{e}^{\mathrm{j}\mathbf{k}(x-x_1)} - \mathrm{j}F_2\,\mathrm{e}^{\mathrm{j}\mathbf{k}(x-x_2)} - F_1\,\mathrm{e}^{\mathbf{k}(x-x_1)} - F_2\,\mathrm{e}^{\mathbf{k}(x-x_2)}),\\ y_3(x) &= \frac{1}{4\mathbf{E}I\mathbf{k}^3}(-\mathrm{j}F_1\,\mathrm{e}^{-\mathrm{j}\mathbf{k}(x-x_1)} - \mathrm{j}F_2\,\mathrm{e}^{-\mathrm{j}\mathbf{k}(x-x_2)} - F_1\,\mathrm{e}^{-\mathbf{k}(x-x_1)} - F_2\,\mathrm{e}^{-\mathbf{k}(x-x_2)}). \end{aligned} \tag{15}$$

The power input at x_1 is

$$\pi_{in1} = \tfrac{1}{2}\,\mathrm{Re}\,(F_1 v_1^*) = \tfrac{1}{2}\,\mathrm{Re}\,(F_1(-\mathrm{j}\omega)y_1^*). \tag{16}$$

When the loss factor is small, $\eta \ll 1$, the complex wavenumber, $\mathbf{k}$, and the complex Young's modulus, $\mathbf{E}$, can be written approximately as [10]

$$\mathbf{k} = k(1 - \mathrm{j}\eta/4), \qquad \mathbf{E} = E(1 + \mathrm{j}\eta). \tag{17}$$

Combining equation (15) with equation (17) and substituting into equation (16) yields

$$\begin{aligned} \pi_{in1} = \frac{1}{2}\frac{\omega}{4EIk^3}\,\mathrm{Re}\,[&F_1F_1^*(1+\mathrm{j})(1+\mathrm{j}\eta/4) + F_1F_2^*(1+\mathrm{j}\eta/4)\,\mathrm{e}^{-\mathrm{j}k(1+\mathrm{j}\eta/4)(x_1-x_2)}\\ &+ \mathrm{j}\,\mathrm{e}^{k(1+\mathrm{j}\eta/4)(x_1-x_2)})], \end{aligned} \tag{18}$$

which can also be expressed as

$$\begin{aligned} \pi_{in1} = \frac{\omega}{4EIk^3}\,\mathrm{Re}\,[&S_{11}(1+\mathrm{j})(1+\mathrm{j}\eta/4) + S_{12}(1+\mathrm{j}\eta/4)\,\mathrm{e}^{-\mathrm{j}k(1+\mathrm{j}\eta/4)(x_1-x_2)}\\ &+ \mathrm{j}\,\mathrm{e}^{k(1+\mathrm{j}\eta/4)(x_1-x_2)})], \end{aligned} \tag{19}$$

This relationship can be extended to the case of N random input forces, for which the power input spectral density at point i can be written as

$$\pi_{in,i} = \frac{\omega}{4EIk^3}\sum_{j=1}^{N}\mathrm{Re}\,[S_{ij}(\omega)\alpha_{ij}], \tag{20}$$

where the correction factor, α_{ij}, is

$$\alpha_{ij} = (1 + \mathrm{j}\eta/4)\,\mathrm{e}^{\mathrm{j}k(1+\mathrm{j}\eta/4)|x_i - x_j|} + \mathrm{j}\,\mathrm{e}^{-k(1+\mathrm{j}\eta/4)|x_i - x_j|}). \tag{21}$$

For plates, a similar approach using cylindrical travelling waves leads to the expression

$$\pi_{in,i} = \frac{1}{8(D\rho h)^{1/2}}\sum_{j=1}^{N}\mathrm{Re}\,[S_{ij}(\omega)\alpha_{ij}], \tag{22}$$

where the correction factor, α_{ij}, is

$$\alpha_{ij} = (1 + \mathrm{j}\eta/2)[\mathrm{H}_0^{(1)}(k(1+\mathrm{j}\eta/4)r_{ij}) - \mathrm{H}_0^{(1)}(\mathrm{j}k(1+\mathrm{j}\eta/4)r_{ij})], \tag{23}$$

and $\mathrm{H}_0^{(1)}$ is the Hankel function of the first kind; r_{ij} is the distance between points i and j. Again, the only approximation involved in the impedance method is that the impedance of an infinite structure is adopted as the impedance at the driving point. Potential errors caused by this approximation are investigated in the next section.

The coherence condition between any two excitation forces is involved in the cross-power spectral density. The ordinary coherence function is defined as [11]

$$\gamma^2 = \frac{|S_{ij}|^2}{S_{ii}S_{jj}}\,. \tag{24}$$

When the two forces are incoherent, then $S_{ij} = 0$ and $\gamma = 0$. When the two forces are perfectly coherent, $|S_{ij}|^2 = S_{ii}S_{jj}$ and $\gamma = 1$. When the two forces are partially coherent, $0 < |S_{ij}|^2 < S_{ii}S_{jj}$ and $0 < \gamma < 1$.

3. THE ENERGY DENSITY RESPONSE

3.1. EXACT ANALYTICAL EXPRESSIONS FOR BEAMS AND PLATES

3.1.1. *The response of beams*

A so-called "exact" formulation for the energy density response of a beam or a plate may be obtained analytically using a modal analysis method. The equation of motion for a transversely vibrating beam with internal losses is

$$EI(1 + \mathrm{j}\eta)\frac{\partial^4 u}{\partial x^4} + \rho A\frac{\partial^2 u}{\partial t^2} = f(x, t), \tag{25}$$

where u is the transverse displacement of the beam. For the multi-beam excitation shown in Figure 1, the force term is

$$f(x, t) = \sum_{i=1}^{N} f_i(t)\delta(x - x_i). \tag{26}$$

The modal superposition approximation yields

$$u(x, t) = \sum_{r=1}^{\infty} u_r(t)\phi_r(x), \tag{27}$$

where ϕ_r is the rth natural mode of the beam and u_r is the magnitude of rth mode. Substituting equations (26) and (27) into equation (25), one obtains

$$(1 - \mathrm{j}\eta)\ddot{u}_r + \omega_r^2 u_r = \frac{q_r(t)}{\rho A}, \tag{28}$$

where

$$q_r(t) = \sum_{i=1}^{N} f_i\phi_r(x_i). \tag{29}$$

The Fourier transform of equation (28), and substitution into equation (27), yields the Fourier transform of the beam displacement,

$$u(x, \omega) = \frac{1}{\rho A}\sum_{r=1}^{\infty}\frac{\phi_r(x)}{\omega_r^2 - \omega^2(1 - \mathrm{j}\eta)}\sum_{i=1}^{N} F_i\phi_r(x_i). \tag{30}$$

Integration of the displacement power spectrum over the frequency range of interest yields the band-limited mean square value of the displacement [12],

$$\overline{u^2(x)} = \frac{1}{\pi}\frac{1}{(\rho A)^2}\sum_{r=1}^{\infty}\sum_{s=1}^{\infty}\phi_r(x)\phi_s(x)\sum_{i=1}^{N}\sum_{i=1}^{N}\phi_r(x_i)\phi_s(x_j)$$

$$\times\ \mathrm{Re}\left[\int_0^{\infty} H_r(\omega)H_s^*(\omega)S_{ij}(\omega)\,\mathrm{d}\omega\right], \tag{31}$$

where the overbar denotes time averaging. If cross-modal terms are neglected, equation (31) takes the simpler form

$$\overline{u^2(x)} = \frac{1}{\pi}\frac{1}{(\rho A)^2}\sum_{r=1}^{\infty}\phi_r^2(x)\sum_{i=1}^{N}\sum_{j=1}^{N}\phi_r(x_i)\phi_r(x_j)\mathrm{Re}\left[\int_0^{\infty}H_r(\omega)]^2 S_{ij}(\omega)\,\mathrm{d}\omega\right], \tag{32}$$

where $H_r(\omega) = 1/[\omega_r^2 - \omega^2(1 - \mathrm{j}\eta)]$.

The total energy response of the beam is the sum of the kinetic energy and the potential energy [3]:

$$e = \tfrac{1}{2}\rho A\overline{v^2(x)} + \tfrac{1}{2}EI\overline{\left(\frac{\partial^2 u}{\partial x^2}\right)^2}, \tag{33}$$

where $v(x)$ is the velocity distribution. Both $v(x)$ and $\partial^2 u/\partial x^2$ may be obtained from $u(x)$.

3.1.2. *The response of plates*

Similarly, expressions for the energy density response of a plate under discrete random excitation may be obtained using modal analysis methods. The mean square value of the transverse displacement is

$$\overline{u^2(x,y)} = \frac{1}{\pi}\frac{1}{(\rho h)^2}\sum_{r=1}^{\infty}\sum_{s=1}^{\infty}\phi_r(x,y)\phi_s(x,y)\sum_{i=1}^{N}\sum_{j=1}^{N}\phi_r(x_i,y_i)\phi_s(x_j,y_j)$$

$$\times\ \mathrm{Re}\left[\int_0^{\infty}H_r(\omega)H_s^*(\omega)S_{ij}(\omega)\,\mathrm{d}\omega\right]. \tag{34}$$

If the cross-modal terms are neglected,

$$\overline{u^2(x,y)} = \frac{1}{\pi}\frac{1}{(\rho h)^2}\sum_{r=1}^{\infty}\phi_r^2(x,y)\sum_{i=1}^{N}\sum_{j=1}^{N}\phi_r(x_i,y_i)\phi_r(x_j,y_j)\mathrm{Re}\left[\int_0^{\infty}H_r(\omega)]^2 S_{ij}(\omega)\,\mathrm{d}\omega\right]. \tag{35}$$

where $H_r(\omega) = 1/[\omega_{mn}^2 - \omega^2(1 - \mathrm{j}\eta)]$.

The kinetic energy of a plate is [3]

$$T = \tfrac{1}{2}\rho h\overline{v^2(x,y)}. \tag{36}$$

The kinetic energy can be calculated readily from the displacement solution. The expression for the potential energy, however, is complicated. In the far field, the kinetic energy and the potential energy are approximately equal, as illustrated in reference [3]. Hence, the total energy will be approximated as twice the kinetic energy in the following, i.e.:

$$e = 2T = \rho h\overline{v^2(x,y)}. \tag{37}$$

3.2. ENERGY DENSITY RESPONSE OBTAINED USING EFA

3.2.1. *Response of beams*

The energy problem corresponding to Figure 1 is illustrated in Figure 4. The beam is simply supported at both ends; thus the flux of energy there is zero. The power input is broadband. Hence, the total energy density may be calculated by integrating the energy density over the frequency range,

$$e_{total} = \int_{\omega_1}^{\omega_2} e \, \mathrm{d}\omega. \tag{38}$$

For numerical implementation, the integral may be replaced by a summation:

$$e_{total} = \sum_{\omega_1}^{\omega_2} e\delta\omega, \tag{39}$$

where e can be obtained by solving the energy flow analysis equation (equation (1)).

For a beam of length L, the energy density e can be assumed to be

$$e = \sum_{r=0}^{\infty} A_r \cos\frac{r\pi x}{L}. \tag{40}$$

The basis function $\cos(r\pi x/L)$ satisfies the energy boundary conditions. The power inputs are calculated from the transfer function method or the impedance method developed in section 2. Using Fourier techniques, the power input can be expanded in terms of the basis function as

$$\pi_{in}(x) = \sum_{r=0}^{\infty} B_r \cos\frac{r\pi x}{L}, \tag{41}$$

where

$$B_r = \int_0^L \pi_{in}(x) \cos\frac{r\pi x}{L} \, \mathrm{d}x. \tag{42}$$

Using equation (1), the energy density is

$$e = \sum_{r=0}^{\infty} \frac{B_r \cos(r\pi x/L)}{(c_g^2/\eta\omega)(r\pi/L)^2 + \eta\omega}. \tag{43}$$

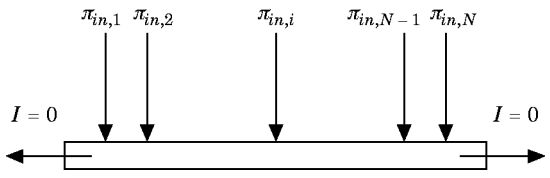

Figure 4. A beam excited by N power inputs.

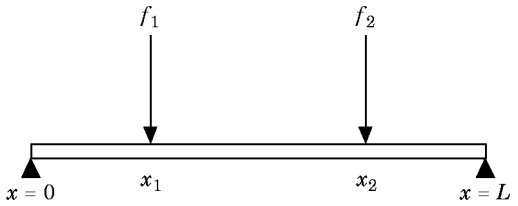

Figure 5. The configuration for the case for the simply supported beam excited by two discrete random forces.

3.2.2. *The response of plates*

For the corresponding plate vibration problems, the energy density calculated by EFA is

$$e = \sum_{m,n=0}^{\infty} \frac{B_{mn} \cos(m\pi x/Lx) \cos(n\pi y/Ly)}{(c_g^2/\eta\omega)[(m\pi/Lx)^2 + (n\pi/Ly)^2] + \eta\omega}, \tag{44}$$

where

$$B_{mn} = \int_0^{Ly} \int_0^{Lx} \pi_{in}(x, y) \cos\frac{m\pi x}{Lx} \cos\frac{n\pi y}{Ly} \, dx \, dy \tag{45}$$

and L_x and L_y are the dimensions of the plate.

4. RESULTS

The accuracy of several aspects of the energy flow analysis approach will be examined in this section. The accuracy of the impedance method will be studied by comparing the computed power input values at point loads with the power inputs calculated using the "exact" transfer function method. The effects of the input force coherence on the power inputs and energy responses will be discussed. The accuracy of the EFA will also be investigated for multiple inputs by comparing the energy density response of beams and plates obtained using the modal analysis method with both EFA solutions.

4.1. BEAMS

For the beam cases, the beam is uniform and simply supported at both ends. Two random forces are acting on the beam, as shown in Figure 5. The auto-spectral densities of the two forces are equal and have a Gaussian distribution. The center frequency is 500 Hz and the half-power bandwidth is 230 Hz, as shown in Figure 6. The mean square value of each force is $5{\cdot}0 \times 10^{-5}$ N^2. The beam parameters are: $E = 7{\cdot}1 \times 10^{10}$ N m^{-2}, $A = 0{\cdot}0001$ m^2, $\rho = 2700$ kg m^{-3}, $I = 8{\cdot}33 \times 10^{-10}$ m^4, $\eta = 0{\cdot}2$ and $L = 1{\cdot}0$ m.

The power inputs were calculated over the frequency range from 0 Hz to 1000 Hz. The frequency range was divided into 200 frequency bands, with a resolution bandwidth of 5 Hz. The power input for each frequency component was calculated using the transfer function method and the impedance method. The total power input was obtained by summing the power input for each frequency component.

In Figure 7, the dependence of the power input on the coherence of the two input forces, $x_1 = 0{\cdot}3$ m and $x_2 = 0{\cdot}7$ m, is shown. The result shown is the power input at position x_1. For these force positions, the "exact" power input increases with coherence. The impedance method captures this trend. The impedance method underestimates the exact result by about 1 dB. The difference between the two power input results decreases with

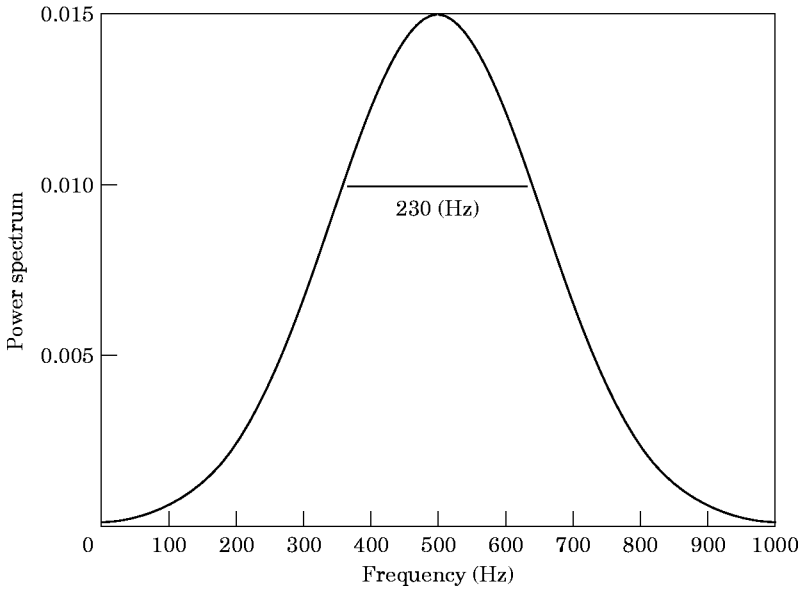

Figure 6. The autospectral density of the forces f_1 and f_2 for the beam case studies.

coherence. In Figure 8, the effects of input force coherence on power inputs when the two force positions are $x_1 = 0{\cdot}4\ m$ and $x_2 = 0{\cdot}6$ m is shown. The result shown is the power input at point x_1. For this situation, the "exact" power input decreases with coherence. The power input when the two forces are completely coherent is about 4 dB lower than the power input when the forces are incoherent. The result by the impedance method also shows this trend. Note that the cross-spectral density always increases with the coherence. Therefore, it is the correction factor in equation (20) that dominates and makes the power input decrease with coherence in this case. It is clearly shown that the effects of coherence

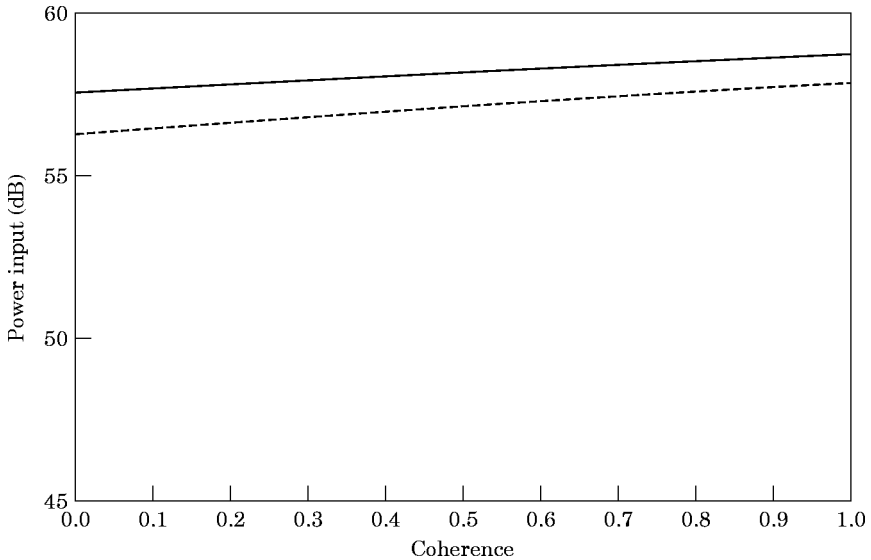

Figure 7. Power input versus input forces coherence for the force positions: $x_1 = 0{\cdot}3$ m, $x_2 = 0{\cdot}7$ m. ——, transfer function method; ----, impedance method. The reference input power is 1×10^{-12} W m^{-2}.

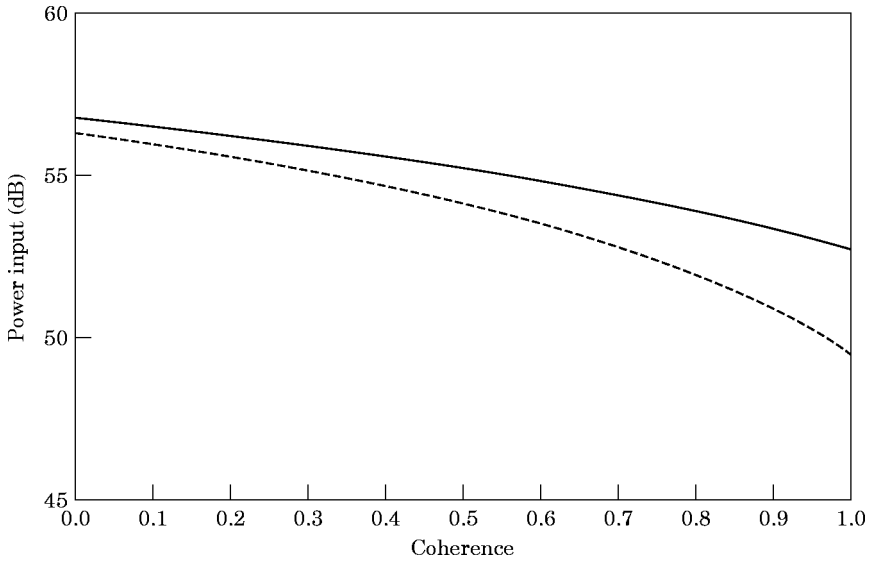

Figure 8. Power input versus input forces coherence for the force positions: $x_1 = 0{\cdot}4$ m, $x_2 = 0{\cdot}6$ m. ——, transfer function method; ----, impedance method. The reference input power is 1×10^{-12} W m^{-2}.

on the power input depends on the force positions. The coherence has a more significant effect when the two force positions are close to each other. The impedance method is consistent with the transfer function method in predicting the effects of coherence and force positions.

The accuracy of the EFA was investigated by comparing the EFA solutions with modal analysis results. The two input force positions are $x_1 = 0{\cdot}3$ m and $x_2 = 0{\cdot}7$ m. For the numerical implementation of the modal analysis method, a total of 70 modes were used to insure satisfactory convergence of the solution. Results were obtained with and without including the cross-modal terms.

For the EFA method, the power inputs were calculated using both the transfer function method and the impedance method. The same frequency range divisions as those used in calculating the power inputs were used for EFA. The energy density for each frequency component was calculated from equation (43). The total energy density response was obtained by summing the energy density for each frequency component using equation (39).

In Figure 9 is shown the energy density response for the case of two incoherent random forces; i.e., $\gamma = 0$. Two of the results shown are obtained using the modal analysis method: one considering the cross-modal terms and one neglecting the cross-modal terms. The other two results are obtained from EFA: one using the transfer method, and the other one using the impedance method.

There is a difference between the two results for the modal analysis method, particularly near the center of the beam. The errors involved, however, are not very significant. There are discrepancies between the modal analysis solutions and the approximate EFA solutions. The energy distribution obtained from EFA is nearly uniform along the beam. It is slightly higher at the two excitation points, and decays away from the excitation. In contrast, the exact energy distribution is non-uniform. This is especially true near the boundaries, where the exact solution tends toward zero (in agreement with the boundary conditions) while the approximate solutions are nearly constant. However, the EFA

solution is a good representation of the spatially averaged response. This result is typical of results found by previous investigators for a harmonic input [2–4]. The difference between the two EFA results is approximately 1 dB. The difference between the power inputs calculated using the transfer function method and the impedance method is approximately 1 dB, as shown in Figure 7. Due to the linear relationship between the power input and the EFA energy density, the difference between the two EFA results is the same as the difference between the power inputs.

The case of two partially coherent forces was also investigated. The coherence between the two random forces, expressed as

$$\gamma = \mathrm{e}^{-0{\cdot}0005\omega|x_1 - x_2|}, \tag{46}$$

was assumed to depend on the distance between the two forces and to decrease with frequency. The energy density distributions computed using the modal analysis method and EFA are shown in Figure 10. Similar results for the case of two perfectly coherent random forces, i.e., $\gamma = 1$, are shown in Figure 11. As the coherence is increased, the effects of the interference between the two random forces become important. This is reflected in the exact results in Figures 9–11. For cases with a higher coherence, the spatial variation of the energy density is increased. The difference between the two EFA results decreases when the coherence increases, because the difference between the two power inputs decreases with coherence. Furthermore, the global energy density response increases with the coherence, as demonstrated by both the modal analysis method and the EFA method. For this case, the power inputs increase with coherence, as shown in Figure 7. For all cases, both EFA solutions are good predictions of the spatially averaged results.

4.2. PLATES

The plate used for the verification study was simply supported along its edges and excited by two random forces located at $(x_1, y_1) = (0{\cdot}3\text{ m}, 0{\cdot}3\text{ m})$ and $(x_2, y_2) = (0{\cdot}7\text{ m}, 0{\cdot}7\text{ m})$, as shown in Figure 12. The auto-spectral densities of the two forces were equal

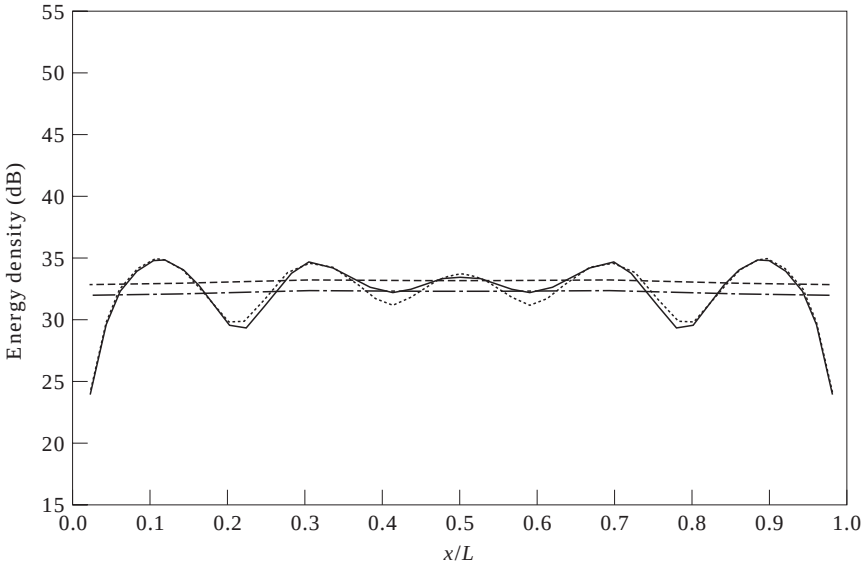

Figure 9. Energy density versus position for the case of two incoherent forces. ——, modal analysis method/considering cross-modal terms; ····, modal analysis method/neglecting cross-modal terms; ----, EFA/transfer function method; –·–·–·–, EFA/impedance method. The reference energy density is 1×10^{-12} J m^{-2}.

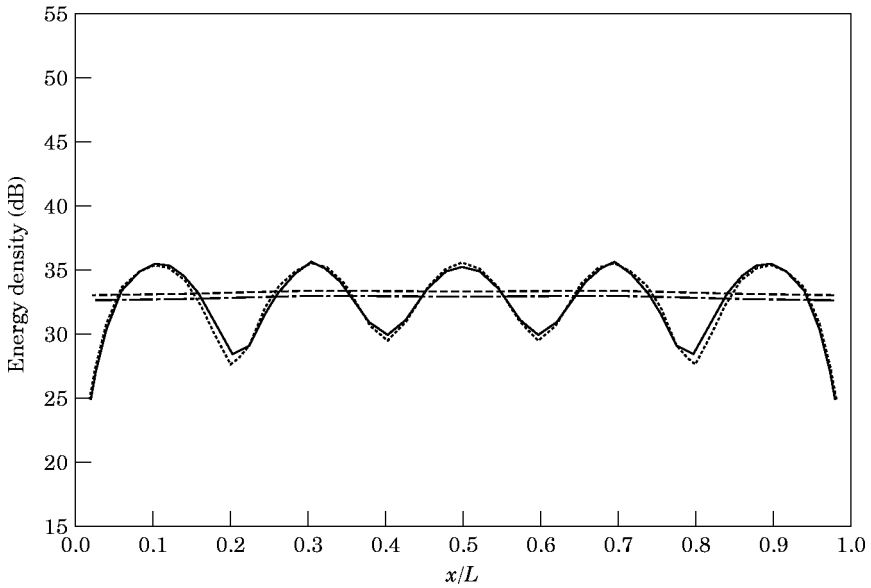

Figure 10. Energy density versus position for the case of two partially coherent forces. ——, modal analysis method/considering cross-modal terms; ····, modal analysis method/neglecting cross-modal terms; ----, EFA/transfer function method; –·–·–·–, EFA/impedance method. The reference energy density is 1×10^{-12} J m^{-2}.

and the same as those for the beam cases. The parameters of the plate were: $E = 7{\cdot}1 \times 10^{10}$ N · m^{-2}, $\rho = 2700$ Kg · m^{-3}, $h = 0{\cdot}001$ m, $L_x = L_y = 1{\cdot}0$ m, $\eta = 0{\cdot}2$ and $\sigma = 0{\cdot}3$.

The power inputs were calculated using both the transfer function method and the impedance method. The power input at point load (x_1, y_1) is shown in Figure 13 for different input force coherence. The power inputs are essentially independent of coherence

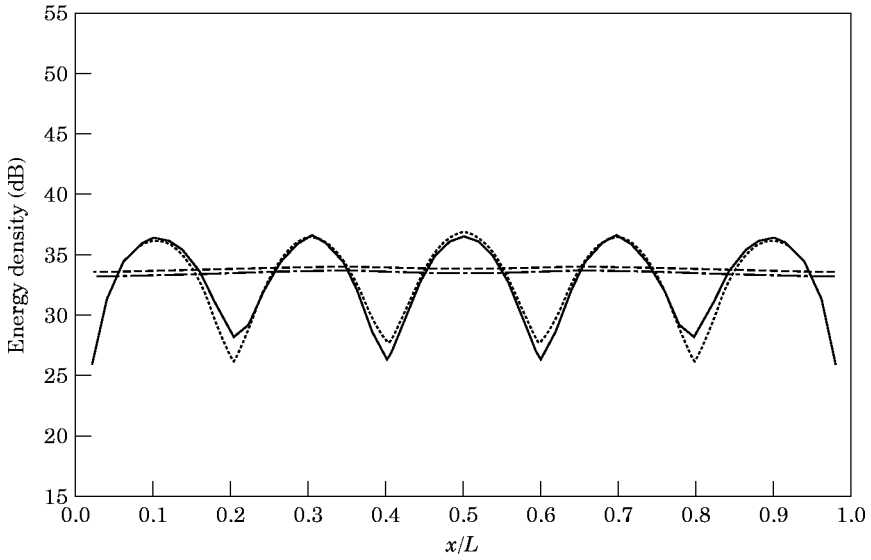

Figure 11. Energy density versus position for the case of two perfectly coherent forces. ——, modal analysis method/considering cross-modal terms; ····, modal analysis method/neglecting cross-modal terms; ----, EFA/transfer function method; –·–·–·–, EFA/impedance method. The reference energy density is 1×10^{-12} J m^{-2}.

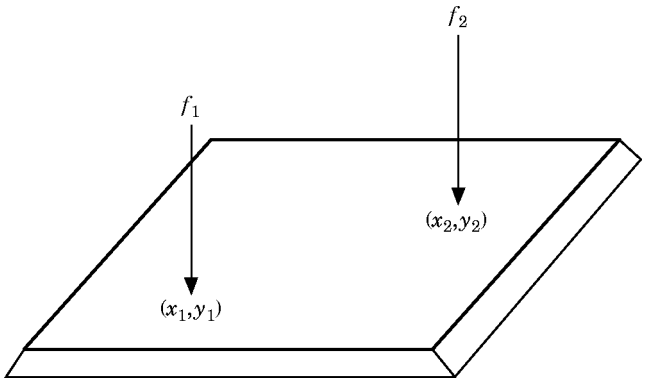

Figure 12. The plate response problem.

in this case, which indicates that, for these specific force positions, the coherence has no effects on power input. The difference between the two results is small. This indicates that the approximate method for calculating the power input using the infinite structure impedance approximation is accurate. This is significant, because the computational effort for calculating the power input to a system is greatly reduced using the impedance approximation. In addition, power input using the transfer function method requires knowledge of the modes of the structure, whereas the impedance method requires only local information. For plates with high modal density, the difference between the results of the two power input methods is much smaller than that for beams, which indicates that the impedance method is more effective for plates than for beams.

The energy density was computed using the modal analysis method, including the cross-modal terms, and EFA. The input power used for EFA was obtained using both the transfer function method and the impedance method. For the modal analysis method, a

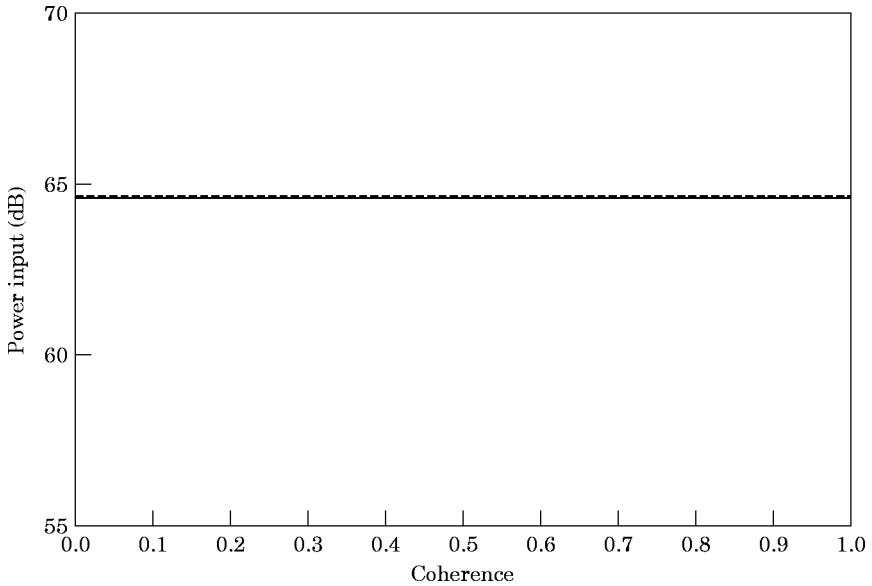

Figure 13. Power input versus input forces coherence for the force positions: $(x_1, y_1) = (0{\cdot}3\text{ m}, 0{\cdot}3\text{ m})$, $(x_2, y_2) = (0{\cdot}7\text{ m}, 0{\cdot}7\text{ m})$. ——, transfer function method; ----, impedance method. The reference input power is $1 \times 10^{-12}\text{ W m}^{-2}$.

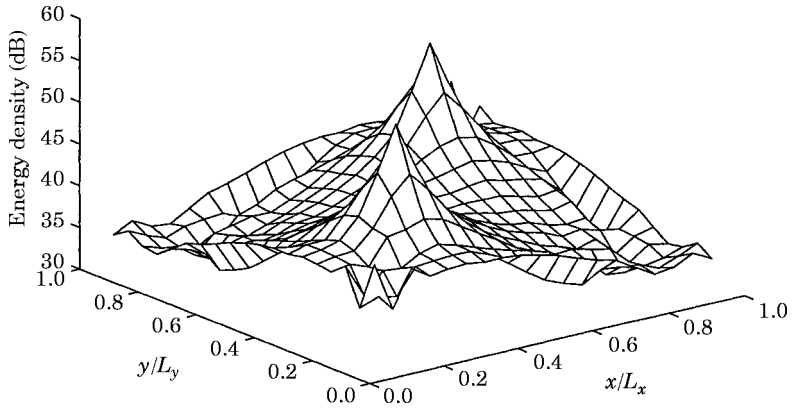

Figure 14. Energy density distribution by modal analysis method for the case of two discrete incoherent random forces. The reference energy density is 1×10^{-12} J m^{-2}.

total of 2500 modes were used, which ensured convergence for this case. For EFA, the energy density was computed over the frequency range from 0 Hz to 1000 Hz. The frequency range was divided into 100 bands with bandwidth 10 Hz.

Three cases were studied for plate vibrations: (1) incoherent forces, (2) partially coherent forces and (3) perfectly coherent forces. The exact energy distribution for case 1 ($\gamma = 0$) is shown in Figure 14. The approximate energy distributions obtained from the transfer function method and the impedance method are shown in Figures 15 and 16, respectively. The differences between the two approximate results are not significant.

For the second case, the coherence between the two random forces was assumed to be given by

$$\gamma = \mathrm{e}^{-0{\cdot}005\omega|x_1 - x_2|}\,\mathrm{e}^{-0{\cdot}02\omega|y_1 - y_2|}; \tag{47}$$

i.e., to decay exponentially as a function of distance between the two forces, and to decrease with frequency at a different rate in the longitudinal and transverse directions. The exact energy density distribution is shown in Figure 17. The EFA solutions computed from the two different power input methods are almost the same as those for the case of

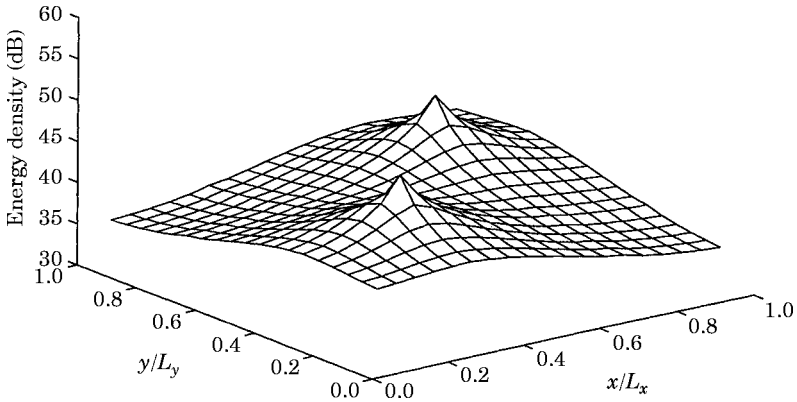

Figure 15. Energy density distribution by EFA/transfer function method for the case of two discrete incoherent random forces. The reference energy density is 1×10^{-12} J m^{-2}.

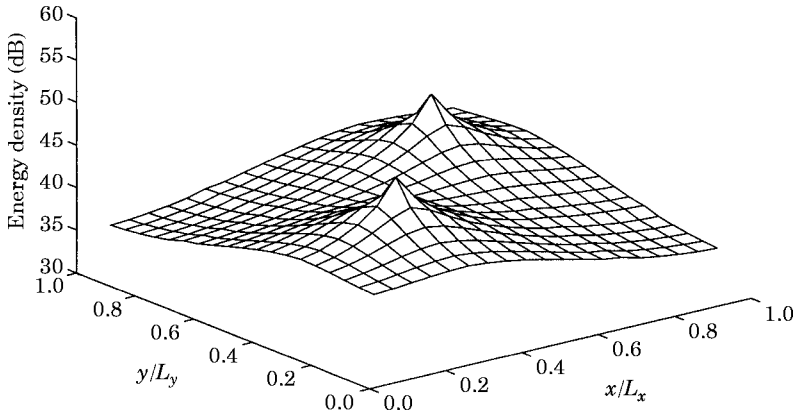

Figure 16. Energy density distribution by EFA/impedance method for the case of two discrete incoherent random forces. The reference energy density is 1×10^{-12} J m^{-2}.

incoherent forces, because the power input is constant with coherence. The results are not shown here for conciseness. For the last case, the two random forces are coherent. The exact result is shown in Figure 18. The two EFA results are very similar to those for the cases of incoherent and partially coherent forces, and therefore are not shown.

In order to illustrate the difference between the exact solutions and the EFA approximations, and to verify the effects of different coherence conditions, the energy response along the diagonal line $x = y$ was plotted for various cases. A comparison of the EFA results computed using different power input methods is shown in Figure 19. The results obtained from the transfer function method and impedance method are in excellent agreement. For these force positions, the coherence has no effect on power inputs, or the EFA energy responses. As discussed above, the power input depends on the positions of the excitation forces. For other excitation positions, the global energy density responses may increase or decrease with coherence.

A comparison between the exact energy density distribution calculated for all three cases is shown in Figure 20, together with the approximate EFA solutions (from Figure 19). In the center of the plate, the energy density responses increase with coherence. This is due

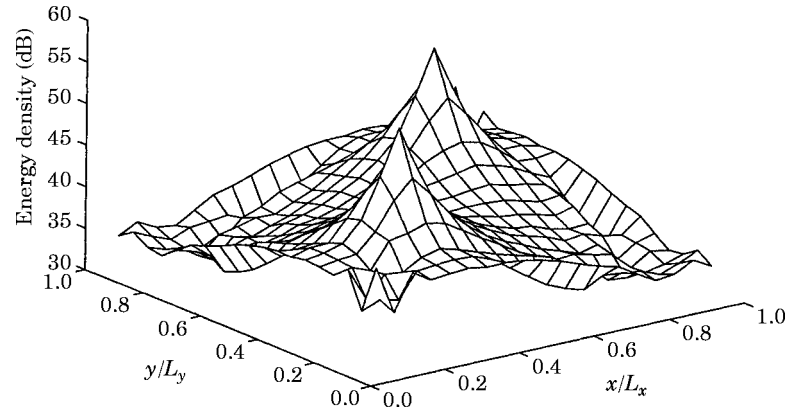

Figure 17. Energy density distribution by modal analysis method for the case of two discrete partially coherent random forces. The reference energy density is 1×10^{-12} J m^{-2}.

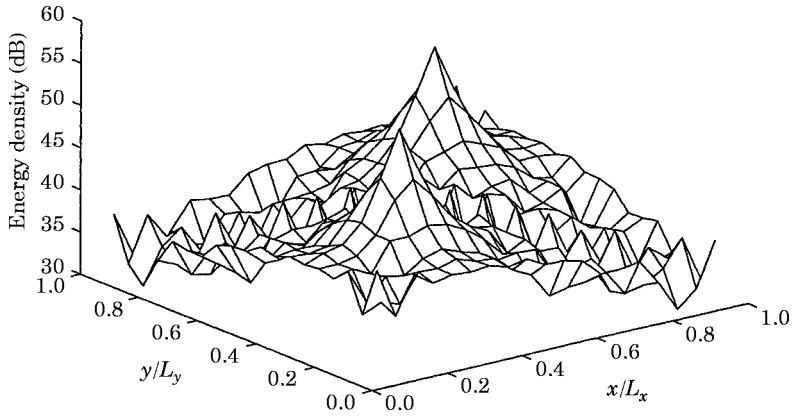

Figure 18. Energy density distribution by modal analysis method for the case of two discrete perfectly coherent random forces. The reference energy density is 1×10^{-12} J m^{-2}.

to constructive interference. However, the effects of coherence are relatively small at the excitation points and near the boundary for these force positions. The exact results monotonically decay from the excitation points, with an increase in energy density close to the boundaries. This is an artifact from the assumption that the potential energy and the kinetic energy are equal, which breaks down close to the plate boundary. In the vicinity of the excitation points, the EFA result is lower than the exact result, whereas in the region close to the boundaries EFA overpredicts the energy response. These trends are typical of EFA results reported in previous studies [2–4], and occur because this particular EFA approximation (assuming lossy plane waves) does not model the near field. A solution to this problem was proposed by Smith [14]. In the area far from the excitation points and the boundary, the EFA result is a good representation of the exact result.

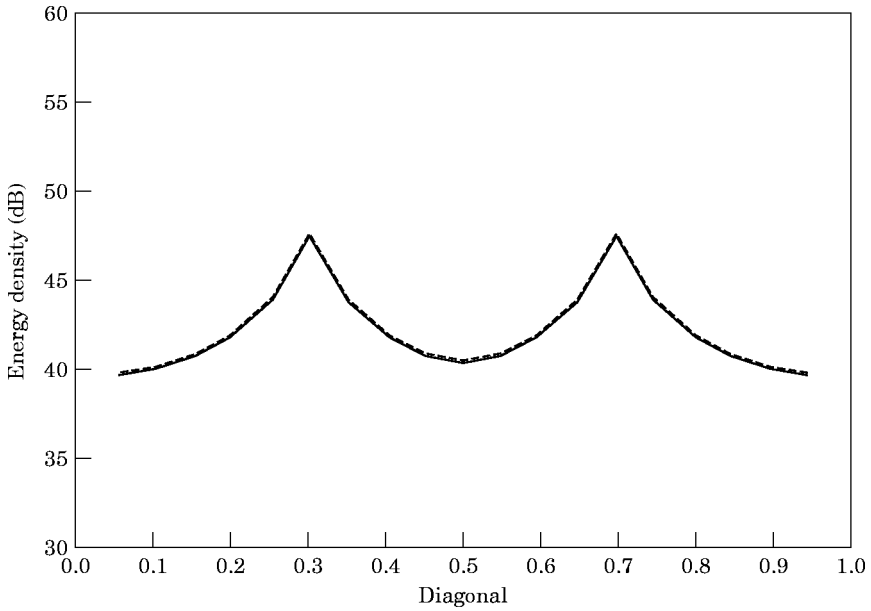

Figure 19. Energy density distribution by EFA along the diagonal: ——, transfer function method; ----, impedance method. The reference energy density is 1×10^{-12} J m^{-2}.

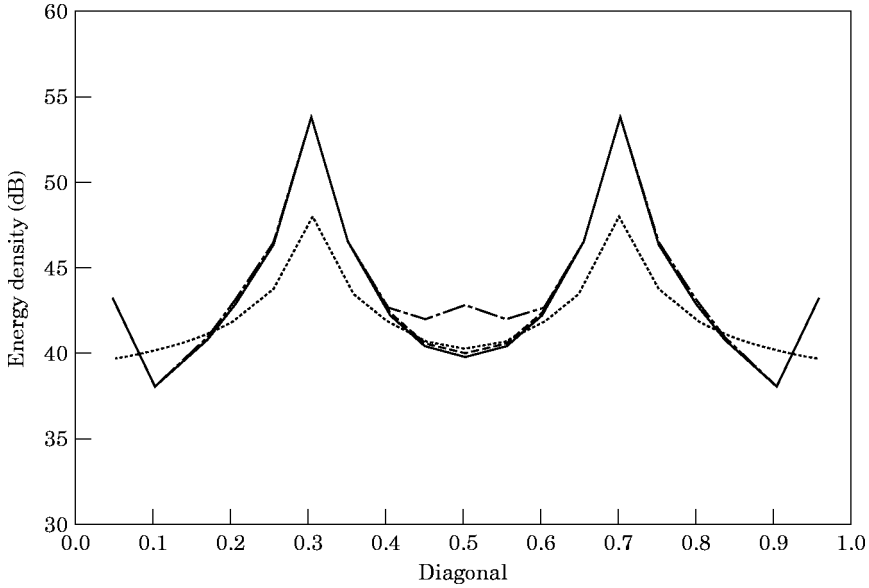

Figure 20. Energy density distribution along the diagonal for the cases of different coherence: ——, incoherent/exact result; ----, partially coherent/exact result; –·–·–·–, coherent/exact result; ····, EFA result. The reference energy density is 1×10^{-12} J m^{-2}.

5. CONCLUSIONS

Two methods for calculating the power input to vibrating beams and plates excited by discrete random forces have been developed: a transfer function method and an impedance method. The power input was expressed in terms of the cross-power spectral density between the excitation forces, thus allowing for the inclusion of the coherence condition in the expressions for the power input. The energy response of simply supported beams and plates was calculated using both power input calculation schemes for different coherence conditions between the excitation random forces. The results showed that the energy flow analysis method can be used to predict the space averaged energy response of a vibrating system under multiple random exciting forces. Results using the impedance method of calculating power inputs were found to be accurate within the accuracy expected for approximate, energy-based models. The methods, can be easily implemented using the finite element method, and are expected to be applicable to many practical engineering problems.

REFERENCES

1. J. C. Wohlever and R. J. Bernhard 1992 *Journal of Sound and Vibration* **153**, 1–19. Mechanical energy flow models of rods and beams.
2. O. M. Bouthier and R. J. Bernhard 1995 *Journal of Sound and Vibration* **182**, 129–147. Simple models of the energy flow in vibrating membranes.
3. O. M. Bouthier and R. J. Bernhard 1995 *Journal of Sound and Vibration* **182**, 149–164. Simple models of the energetics of transversely vibrating plates.
4. O. M. Bouthier 1992 *Ph.D. Thesis*, *Purdue University*. Energetics of vibrating systems.
5. S. A. Rybak 1972 *Journal of Soviet Phyics—Acoustics* **17**, 345–349. Waves in a plate containing random inhomogeneities.
6. S. A. Rybak 1972 *Journal of Soviet Phyics—Acoustics* **18**, 76–79. Randomly coupled flexural and longitudinal vibrations of plates.

7. V. D. Belov and S. A. Rybak 1975 *Journal of Soviet Phyics—Acoustics* **23**, 110–114. Applicability of the transport equation in one-dimensional wave-propagation problem.
8. V. D. Belov, S. A. Rybak and B. D. Tartakovskii 1977 *Journal of Soviet Physics—Acoustics* **23,** 115–119. Propagation of vibrational energy in absorbing structures.
9. A. Lebot and L. Jezequel 1993 *Proceedings of the* 4*th International Congress on Intensity Techniques*, *Senlis* (*France*), 371–378. Energy methods applied to transverse vibrations of beams.
10. F. Fahy 1985 *Sound and Structural Vibration*: *Radiation*, *Transmission*, *and Response*. London: Academic Press.
11. J. S. Bendat and A. G. Piersol 1986 *Random Data Analysis and Measurement Procedures*. New York: John Wiley.
12. S. H. Crandall and W. D. Mark 1963 *Random Vibration in Mechanical Systems*. London: Academic Press.
13. L. Cremer and M. Heckl 1988 *Structure-borne Sound*. New York: Springer Verlag.
14. M. J. Smith 1997 *Journal of Sound and Vibration* **202**, 375–394. A hybrid energy method for predicting high frequency vibrational response of point-loaded plates.